

DNMT1 facilitates proliferation and metastasis of breast cancer cells by promoting MEG3 promoter methylation in MEG3/miR-494-3p/OTUD4 regulatory axis

Xiaotao Zhu

Jinhua Municipal Central Hospital

Lin Lv

Jinhua Municipal Central Hospital

Mingzheng Wang

Jinhua Municipal Central Hospital

Chen Fan

Women and Children Branch of Jinhua Municipal Central Hospital

Xiaofeng Lu

Jinhua Municipal Central Hospital

Miaomiao Jin

Jinhua Municipal Central Hospital

Shuguang Li

Jinhua Municipal Central Hospital

Fan Wang (✉ wangfan0997@163.com)

Jinhua Municipal Central Hospital <https://orcid.org/0000-0003-4643-0500>

Primary research

Keywords: DNMT1, MEG3, miR-494-3p, OTUD4, methylation, breast cancer, proliferation, migration and invasion

Posted Date: May 27th, 2020

DOI: <https://doi.org/10.21203/rs.3.rs-27423/v1>

License:   This work is licensed under a Creative Commons Attribution 4.0 International License.

[Read Full License](#)

Abstract

Background

To explore the mechanism of DNMT1 facilitating proliferation and metastasis of breast cancer cells by promoting MEG3 promoter methylation in MEG3/miR-494-3p/OTUD4 regulatory axis.

Methods

Human breast cancer cell lines (MCF-7, MDA-MB-231, SKBR3) and human breast epithelial cell line MCF10A were selected for the experiments. The expressions of DNMT1, MEG3, miR-494-3p and OTUD4 were detected by qRT-PCR. Western blot was used to detect the protein expressions of DNMT1 and OTUD4. CHIP assay verified the binding relationship of DNMT1 and MEG3 promoter region. MEG3 methylation and its level were test by MethPrimer software and MSP, respectively. The targeted binding sites of miR-494-3p and MEG3/OTUD4 were predicted by bioinformatics. RIP and dual-luciferase reporter gene assays verified the combination of miR-494-3p and MEG3/OTUD4. Cell proliferation, migration and invasion abilities were detected by CCK-8, wound healing and Transwell assays.

Results

DNMT1 was highly expressed while MEG3 was poorly expressed in breast cancer cells. Silencing DNMT1 inhibited the proliferation, migration and invasion of breast cancer cells by promoting the expression of lncRNA MEG3 through demethylation. MEG3 as a ceRNA regulated the expression of miR-494-3p in breast cancer. In addition, miR-494-3p could bind to the 3'-UTR of OTUD4, thus negatively regulating the expression of OTUD4 and forming the MEG3/miR-494-3p/OTUD4 regulatory axis that affected the proliferation, invasion and migration of breast cancer. Overexpression of MEG3 could inhibit breast cancer tumor growth *in vivo*.

Conclusion

Silencing DNMT1 promoted the expression of MEG3 through demethylation, which inhibited the expression of miR-494-3p to promote the expression of downstream target OTUD4, thus inhibiting the proliferation, migration and invasion abilities of breast cancer cells.

Highlights

- 1. Silencing DNMT1 promotes the expression of lncRNA MEG3 through demethylation, thus inhibiting the proliferation, migration and invasion abilities of breast cancer cells.**
- 2. miR-494-3p is the target of MEG3 in breast cancer cells.**

3. Silencing miR-494-3p can promote the expression of OTUD4 and inhibit the proliferation, migration and invasion of breast cancer cells.

Background

Breast cancer is one of the most common aggressive malignancies with the highest incidence and remains the first cause of cancer death in women worldwide, leading to 522,000 deaths since 2008¹. Like other solid tumors, distant metastasis (especially lung metastasis) is a major cause of breast cancer-related deaths and resistance to various treatments breast cancer².

DNA hypermethylation is a major epigenetic feature that distinguishes cancer cells from normal cells, which causes insensitivity of cancer cells to growth inhibitory signals and evades programmed cell death by inhibiting tumor-suppressor genes³. DNA hypermethylation is involved in the occurrence and cell survival of breast cancer, and its initiation mechanism is the abnormal expression of DNA methyltransferases (DNMTs), including DNMT1, DNMT3a and DNMT3b⁴⁻⁶. DNMT1 is an important methyltransferase being high in dividing cells compared with nondividing cells and has become the main therapeutic target for methylation inhibition in tumor cells⁷. The downregulation of DNMT1 has been reported to inhibit the proliferation and invasion of breast cancer cells⁸. DNMT1 can downregulate maternally expressed gene 3 (MEG3) expression through increasing methylation level of MEG3 in breast cancer⁹. MEG3 has been identified as an imprinted gene with maternal expression and encodes a long non-coding RNA (lncRNA)¹⁰. MEG3 is closely related to the occurrence and development of breast cancer and studies have shown that overexpression of MEG3 can induce growth stagnation and increase apoptosis of breast cancer cells¹¹. Meanwhile, overexpression of MEG3 suppresses breast cancer cell proliferation, invasion and angiogenesis through AKT pathway¹².

In addition, many studies have shown that lncRNAs functions as competitive endogenous RNAs (ceRNAs) sponging miRNA and regulating the expression of miRNA targets^{13,14}. It has been reported that lncRNA MEG3 inhibits cell epithelial-mesenchymal transition (EMT) by targeting miR-421 and regulating E-cadherin in breast cancer¹⁵. High expression of miR-494-3p has an inhibitory effect on breast cancer by targeted down-regulating TRIM21. But there is no report on MEG3 as a ceRNA regulating the expression of miR-494-3p in breast cancer. In addition, the targets of miR-494-3p were also studied.

In this study, we investigated the effects of DNMT1 on MEG3 methylation and the MEG3/miR-494-3p/OTUD4 regulatory axis on the proliferation, migration and invasion of breast cancer, which could help develop treatment strategies for breast cancer.

Materials And Methods

Bioinformatics analysis

RAID database (<http://www.rna-society.org/raid2/index.html>) and starBase database (<http://starbase.sysu.edu.cn/>) were used to obtain downstream regulatory miRNAs of MEG3 and the potential targeted binding sites of lncRNA-miRNA. GSE70905 dataset of breast cancer was obtained through GEO database, including 45 normal samples and 45 tumor samples. Normal samples were taken as control and the differential analysis was conducted using "limma" package in R language. *P*-value was corrected by using FDR method. Differentially expressed genes (DEGs) were screened with $|\log_{2}FC| > 1$ and *p* value < 0.05 . The downstream target genes of miR-494-3p were predicted by TargetScan (http://www.targetscan.org/vert_71/), mirDIP (<http://ophid.utoronto.ca/mirDIP/index.jsp#r>) and starBase databases (<http://starbase.sysu.edu.cn/>). Targeted binding sites of miRNA-mRNA were obtained by TargetScan database.

Cell culture and transfection

Human breast epithelial cell line MCF10A (NO. 3111C0001CCC000406) human breast cancer cell lines MCF-7 (NO. 3142C0001000001079), MDA-MB-231 (NO. 3111C0001CCC000014), SKBR3 (NO. 3142C0001000000313), and human embryonic kidney cell line HEK-293 (NO. 3111C0001CCC000010) were selected for the experiments. MCF10A, MDA-MB-231 and HEK-293 cells were purchased from the cell resource center of Institute of Basic Medical Sciences, Chinese Academy of Medical Sciences. MCF-7 and SKBR3 cells were purchased from cell bank of China Center for Type Culture Collection. MCF10A, MCF-7 as well as HEK-293, MDA-MB-231 and SKBR3 cells were simultaneously cultured in DMEM-F12 medium, MEM-EBSS medium (MEM Eagles with Earle's Balanced Salts), L15 medium (Leibovitz Medium) and McCoy's 5A Media medium (Modified with Tricine), respectively. The mediums were all purchased from Hyclone and contained 10% FBS.

Lentivirus vector construction

MEG3 cDNA was cloned into pcDNA4 vector, while DNMT1 shRNA, MEG3 shRNA and OTUD4 shRNA were cloned into PLKO.1 vectors. pPAX2 and pVSVG along with target vectors were co-transfected into 293T cells. Supernatant was harvested at 24 h and 48 h after transfection and filtered through 0.45 μ m membrane. The viral supernatant was added to the medium in a ratio of 1:3 for viral infection. After 24 h, stably transfected cell lines were selected using 2 μ g/ml puromycin. All vectors, miR-494-3p mimic/inhibitor and their corresponding controls were purchased from GenePharma (Shanghai, China). The scramble shRNA and empty pcDNA4 vector were used as negative controls, respectively.

Dual-luciferase reporter gene assay

The 3'-UTR of MEG3 or OTUD4 was ligated to psiCHECK2 vector that was fused with luciferase gene and had been digested with XhoI and NotI restriction enzymes. The QuikChange multi-site-directed Mutagenesis kit (Stratagene, LaJolla, CA) was used to mutate the targeted sites of miR-494-3p on 3'-UTR. Luciferase activities were determined by dual-luciferase assay (Promega) and Renilla luciferase activity was used for normalization of firefly luciferase activity.

RNA binding protein immunoprecipitation (RIP) assay

RIP was performed using the Magna RIP RNA-Binding Protein Immunoprecipitation kit (Millipore, Burlington, MA). MDA-MB-231 cells in each group were lysed. Then the whole cell lysates were cultured with protein magnetic beads and incubated with 2 µg of Ago2 antibody (ab186733, 1:30, Abcam, UK) or control IgG (ab205718, 1:50, Abcam, UK) overnight at 4 °C. The immunoprecipitated RNA was purified and the expressions of MEG3, miR-494-3p and OTUD4 were detected by qRT-PCR.

Chromatin immunoprecipitation (ChIP) assay

Enrichment of DNMT1 in MEG3 promoter region was analyzed using ChIP kit (Millipore, USA). When the MDA-MB-231 cells were grown to 70–80% in confluence, 1% formaldehyde was added to the cells and cells were fixed at room temperature for 10 min to make the DNA and proteins in the cells immobilized and cross-linked. Then the cross-linked products were randomly fragmented into fragments of appropriate size by 10 s of ultrasonication for 15 cycles with an interval of 10 s. After centrifugation at 13000 rpm at 4 °C, the collected supernatant was divided into 3 tubes and cultured with positive control antibody RNA polymerase II, negative control antibody IgG of normal mice (ab6721, 1:30, Abcam, UK) and methylation transferase specific antibody DNMT1 (ab13537, 1:50, Abcam, UK) overnight at 4 °C, respectively. Protein Agarose/Sepharose was used to precipitate endogenous DNA-protein complexes, and the supernatant was adsorbed after a short centrifugation. The non-specific complexes were washed and de-crosslinked overnight at 65 °C. The DNA fragments were extracted and purified by phenol/chloroform. qPCR was used to test the combination of DNMT1 and MEG3 promoter region.

Methylation-specific PCR (MSP)

Genomic DNA was treated with sodium bisulfite and DNA methylation was tested by MSP using EZ DNA MethylationDirect kit (Zymo Research). The two primer groups were used to amplify the promoter region of MEG3 containing multiple CpG sites, and the primer sequences were shown in Table 1. PCR reaction conditions: pre-denaturation at 95 °C for 10 min, followed by 35 cycles of 95 °C for 45 s, 56 °C (methylation)/45 °C (non-methylation) for 45 s and 72 °C for 45 s. Finally, it was extended at 72 °C for 10 min. The reaction products were subjected to agarose gel electrophoresis and images were captured for further analysis.

Western blot

RIPA lysis buffer (Takara Biotechnology, Dalian, China) was used to extract total proteins from cells. A total of 20 µg proteins were isolated by 12% sodium dodecyl sulfate-polyacrylamide gel electrophoresis (SDS-PAGE) and transferred onto polyvinylidene fluoride (PVDF) membranes (Millipore Corp., Billerica, MA, USA). After blocked in the TBS buffer containing 5% skim milk (50 mmol/L NaCl, 10 mmol/L Tris, pH7.4), the membranes were washed with TBST for three times at 5 min each time and incubated with the primary antibodies at 4 °C overnight. Primary antibodies were DNMT1 (ab188453, 1:1000, Abcam, UK), OTUD4 (ab106368, 1:500, Abcam, UK) and GAPDH (ab181602, 1:10,000, Abcam, UK). Then, the membranes were washed with TBST as above procedures, and incubated with horseradish peroxidase-conjugated secondary antibody (Santa Cruz Biotechnology) at room temperature for 1 h. Finally, immunoreactive proteins were treated with enhanced chemiluminescence reagent (Amersham, Little

Chalfont, UK) and protein bands were observed using Amersham Imager 600 system (GE Healthcare Life Sciences, Shanghai, China).

qRT-PCR

TRIzol reagent (Invitrogen) was used to extract total RNA from cells, and the OD_{260/280} value of each RNA sample was determined by UV spectrometer. RNA concentrations were calculated and samples were stored at -80 °C for subsequent experiments. Total RNA was extracted using RNeasy Mini Kit (Qiagen, Valencia, CA, USA). cDNA of mRNA was obtained by reverse transcription Kit (RR047A, Takara, Japan). miRNA First Strand cDNA Synthesis kit (B532451-0020, Shanghai Sangon Biotech, China) was used for reverse transcription to obtain cDNA of miRNA. The samples were loaded using the SYBR® Premix Ex Taq™ II (Perfect Real Time) kit (DRR081, Takara, Japan) and subjected to qRT-PCR reaction in a real-time fluorescence quantitative PCR instrument (ABI 7500, ABI, Foster City, CA, USA). The PCR amplification procedure was set pre-denaturation at 95 °C for 30 s, followed by 40 cycles of 95 °C for 5 s and 60 °C for 34 s. Each sample treatment was repeated in triplicate. Primers were synthesized by Shanghai Sangon Biotech Company (Table 1). Ct value of each well was recorded with GAPDH or U6 as internal reference. The relative expression was calculated by $2^{-\Delta\Delta Ct}$ method. $\Delta\Delta Ct = (\text{average Ct value of target gene in experimental group} - \text{average Ct value of housekeeping gene in experimental group}) - (\text{average Ct value of target gene in control group} - \text{average Ct value of housekeeping gene in control group})$.

CCK-8

Cell proliferation was assessed by cell counting kit-8 (CCK-8; Beyotime Biotechnology, China). 3×10^3 MDA-MB-231 cells were inoculated into 96-well plates. After transfection on day 1, day 2, day 3 and day 4, 10 μ l of CCK-8 reagent was added to each well. The plates were placed at 37 °C for 2 h, and the absorbance was read at 450 nm using a microplate reader (Bio-Rad, San Diego, CA, USA). The absorbance value was expressed as a percentage of the experimental group to the control group.

Wound healing assay

Cell migration was measured by *in vitro* wound healing assay. In brief, 2×10^5 MDA-MB-231 cells were inoculated on 6-well plates and incubated in appropriate complete medium at 37 °C for 16 h. The monolayer was scraped and cells were cultured in a fresh medium without FBS for 24 h. Finally, three different fields were observed and photographed under an inverted microscope to measure the scratch width. Relative scratch width = 24 h scratch width/0 h scratch width.

Transwell invasion assay

The cell invasion was determined using 8.0 μ m Millipore Transwell chambers containing Matrigel. 1×10^5 MDA-MB-231 cells were resuspended in 200 μ l medium without FBS and then inoculated into the upper chambers. Next, 500 μ l medium containing 10% FBS was added to the lower chambers. After 48 h of culture, uninvaded cells were removed from the upper surface of the membranes with a cotton swab, and

the invaded cells were fixed and stained with crystal violet. Finally, 5 randomly selected fields were observed under an inverted microscope to calculate cell number.

Nude mice experiment¹⁶

10 6-week-old BALB/female nude mice were purchased from Beijing HFK bio-technology (Beijing, China). Mice were randomly divided into two groups with 5 in each group. 5×10^6 MDA-MB-231 cells in the sh-NC group and sh-DNMT1 group were resuspended in 100 μ l PBS and then injected into each mouse by tail vein injection. After mice were fed for 5 days, tumor volume was measured by a caliper every 5 days and calculated as follows: $V = D \times d^2 \times 0.5$ (D, longer diameter; d, shorter diameter). After 35 days, the mice were euthanized by CO₂ inhalation. This experiment was approved by the animal care and use committee of Jinhua Municipal Central Hospital.

Statistical analysis

All data were processed by SPSS 21.0 statistical software (SPSS, Inc., Chicago, IL, USA), and the measurement data were expressed as mean \pm standard deviation. The comparison between two groups was analyzed by Students' *t* test, and the comparison among multiple groups was analyzed by one-way ANOVA. $P < 0.05$ indicated the difference was statistically significant.

Results

Silencing DNMT1 inhibits the proliferation, migration and invasion of breast cancer cells by promoting the expression of MEG3 through demethylation

Current studies have found that lncRNA MEG3 is regulated by DNMT1, and the promoter of MEG3 is methylated under the influence of DNMT1, while MEG3 appears to be hypermethylated and lowly expressed in tumors^{9,15,17}. We further examined the effect of the interaction of MEG3 and DNMT1 on the breast cancer cells. DNMT1 and MEG3 expressions in human breast cancer cell lines MCF-7, MDA-MB-231, SKBR3 and the human breast epithelial cell line MCF10A were tested by western blot (Fig. 1A) and qRT-PCR (Fig. 1B), respectively. The results showed that protein expression of DNMT1 was significantly higher, while MEG3 was significantly lowly expressed in breast cancer cells ($P < 0.05$). MDA-MB-231 cell line with the lowest MEG3 expression was chosen for subsequent experiments. ChIP assay was used to detect whether DNMT1 could bind to MEG3 promoter region (Fig. 1C). Compared with IgG control group, DNMT1 enrichment in MEG3 promoter region was significantly increased ($P < 0.05$). CpG islands were found in the MEG3 gene promoter region by analyzing 2100 bp nucleotide sequences near the MEG3 gene promoter region through MethPrimer software, indicating that MEG3 expression would be affected by promoter methylation (Fig. 1D). Then DNMT1 interference efficiency in MDA-MB-231 cells was detected by western blot (Fig. 1E), and sh-DNMT1-1 with the best interference efficiency was selected for subsequent experiments. MEG3 methylation level detected by MSP was shown in Fig. 1F. MEG3 methylation level was significantly decreased and MEG3 expression detected by qRT-PCR was remarkably

up-regulated when silencing DNMT1 (Fig. 1G) ($P < 0.05$). It indicated that silencing DNMT1 could promote MEG3 expression by inhibiting MEG3 promoter methylation.

It has been reported that DNMT1 can promote the proliferation, migration and invasion abilities of breast cancer cells⁸, and MEG3 can inhibit these abilities in breast cancer¹². While in the present study, we identified that DNMT1 could potentiate MEG3 promoter methylation in turn inhibiting MEG3 expression. Based on the above results, we proposed the hypothesis that DNMT1 regulated the proliferation, migration and invasion abilities of breast cancer cells by inhibiting MEG3 expression. The expression of MEG3 was further interfered to explore the effect of DNMT1/MEG3 interaction on breast cancer cells. sh-MEG3-1 with the best interference efficiency directed by qRT-PCR was selected for subsequent experiments (Fig. 1H) ($P < 0.05$). The expressions of DNMT1 and MEG3 in three groups (sh-NC + sh-NC, sh-DNMT1 + sh-NC, sh-DNMT1 + sh-MEG3) were detected by qRT-PCR (Fig. 1I). The expression of DNMT1 was significantly down-regulated ($P < 0.05$) while the expression of MEG3 was remarkably up-regulated in sh-DNMT1 + sh-NC group relative to the sh-NC + sh-NC group ($P < 0.05$). MEG3 expression was obviously down-regulated ($P < 0.05$), but there was no significant difference in DNMT1 expression when DNMT1 and MEG3 were both silenced ($P > 0.05$). Then, the results of CCK-8 (Fig. 1J), wound healing (Fig. 1K) and Transwell (Fig. 1L) assays displayed that silencing DNMT1 decreased cell activity, migration and invasion abilities while these abilities were increased when DNMT1 and MEG3 were silenced simultaneously ($P < 0.05$). In conclusion, silencing DNMT1 inhibited the proliferation, migration and invasion abilities of breast cancer MDA-MB-231 cells by up-regulating MEG3.

miR-494-3p is a target of MEG3 in breast cancer cells

In addition, many studies have pointed out that MEG3 can play a regulatory role by acting as a ceRNA^{18,19}. Further prediction of the downstream regulatory miRNAs of MEG3 (Fig. 2A) found that miR-494-3p could targeted bind to MEG3 (Fig. 2B). Moreover, a study has indicated that the expression level of miR-494-3p in tumors is significantly increased²⁰. Therefore, RIP was used to detect the binding relationship between MEG3 and miR-494-3p (Fig. 2C). Compared with IgG, the number of MEG3 and miR-494-3p bound by Ago2 were significantly increased. Dual-luciferase reporter gene assay verified the targeted binding sites of miR-494-3p on MEG3 3'-UTR (Fig. 2D). It was observed that overexpression of miR-494-3p significantly decreased the relative luciferase activity in the MEG3-wt group ($P < 0.05$) but had no effect in the MEG3-mut group ($P > 0.05$). The expressions of MEG3 and miR-494-3p in the oe-NC group and oe-MEG3 group were detected by qRT-PCR (Fig. 2E). The expression of miR-494-3p was remarkably down-regulated when MEG3 was overexpressed ($P < 0.05$), indicating that MEG3 targeted and negatively regulated miR-494-3p.

Then, rescue experiments were conducted to study the regulation of the MEG3/miR-494-3p interaction on breast cancer. Firstly, the expressions of MEG3 and miR-494-3p in 3 groups (oe-NC + NC mimic group, oe-MEG3 + NC mimic group and oe-MEG3 + miR-494-3p mimic group) were detected by qRT-PCR (Fig. 2F). Overexpression of MEG3 significantly down-regulated miR-494-3p expression, but when MEG3 and miR-494-3p were overexpressed simultaneously, miR-494-3p expression was increased greatly ($P < 0.05$). The

results of CCK-8 (Fig. 2G), wound healing (Fig. 2H) and Transwell (Fig. 2I) assays displayed that overexpression of MEG3 decreased cell activity, migration and invasion abilities while these abilities were increased when MEG3 and miR-494-3p were overexpressed at the same time ($P < 0.05$).

Silencing miR-494-3p can inhibit proliferation, migration and invasion of breast cancer cells by targeted promoting OTUD4 expression

Furthermore, DEGs in breast cancer dataset GSE70905 that was included in GEO database were analyzed (Fig. 3A), and downstream target genes of miR-494-3p were predicted. It was found that OTUD4 was targeted by miR-494-3p and lowly expressed in breast cancer (Fig. 3B-D). Firstly, RIP results shown in Fig. 3E revealed that compared with IgG, the number of miR-494-3p and OTUD4 bound by Ago2 were significantly increased. Dual-luciferase assay verified the targeted binding relationship between miR-494-3p and OTUD4 3'-UTR (Fig. 3F). The result showed that overexpression of miR-494-3p significantly decreased the relative luciferase activity of the OTUD4-wt group ($P < 0.05$) but had no effect in the OTUD4-mut group ($P > 0.05$). OTUD4 expression in NC inhibitor and miR-494-3p inhibitor groups was tested by western blot (Fig. 3G) and the results suggested that silencing miR-494-3p significantly up-regulated OTUD4 expression ($P < 0.05$).

The rescue experiments were also used to detect the regulatory effect of miR-494-3p/OTUD4 on breast cancer. Firstly, sh-OTUD4-1 with the best interference efficiency which was detected by western blot was chosen for subsequent experiments (Fig. 3H). The expressions of miR-494-3p and OTUD4 in 3 groups (NC inhibitor + sh-NC group, miR-494-3p inhibitor + sh-NC group, and miR-494-3p inhibitor + sh-OTUD4 group) were detected by qRT-PCR (Fig. 3I). Silencing miR-494-3p significantly up-regulated OTUD4 expression, but when MEG3 and miR-494-3p were silenced simultaneously, OTUD4 expression increased greatly ($P < 0.05$). The results of CCK-8 (Fig. 3J), wound healing (Fig. 3K) and Transwell (Fig. 3L) assays demonstrated that silencing miR-494-3p decreased cell activity, migration and invasion abilities while the results were opposite when miR-494-3p and OTUD4 were silenced at the same time ($P < 0.05$).

MEG3 negatively regulates miR-494-3p to promote OTUD4 expression and inhibit the proliferation, migration and invasion of breast cancer cells

In order to deeply understand the influence of MEG3/miR-494-3p/OTUD4 as the regulatory axis in breast cancer, the expressions of MEG3, miR-494-3p and OTUD4 in 3 groups (oe-NC + sh-NC group, oe-MEG3 + sh-NC group and oe-MEG3 + sh-OTUD4 group) were detected by qRT-PCR (Fig. 4A), and the protein expression of OTUD4 was detected by western blot (Fig. 4B). Overexpression of MEG3 significantly increased OTUD4 protein and mRNA expressions ($P < 0.05$), but reduced miR-494-3p expression ($P < 0.05$). Compared with oe-MEG3 + sh-NC group, the mRNA and protein expressions of OTUD4 were greatly down-regulated in oe-MEG3 + sh-OTUD4 group ($P < 0.05$), while the expressions of MEG3 and miR-494-3p had no significant difference ($P > 0.05$). The results of CCK-8 (Fig. 4C), wound healing (Fig. 4D) and Transwell (Fig. 4E) assays indicated that overexpression of MEG3 decreased cell activity, migration and invasion abilities ($P < 0.05$) and silencing OTUD4 in MEG3-overexpressing cells could partially alleviate the inhibition ($P < 0.05$).

Overexpression of MEG3 inhibits the tumorigenic ability of breast cancer in vivo

Finally, we overexpressed MEG3 in nude mice to observe the effect of MEG3 on the tumorigenicity of breast cancer. The tumor volume and weight of each group were measured as shown in the Fig. 5A-C. Overexpression of MEG3 reduced tumor volume and weight ($P < 0.05$). The expressions of DNMT1, MEG3, miR-494-3p and OTUD4 were detected by qRT-PCR (Fig. 5D). The protein expressions of DNMT1 and OTUD4 were detected by western blot (Fig. 5E). The results exhibited that miR-494-3p was significantly down-regulated, and MEG3 and OTUD4 were remarkably up-regulated ($P < 0.05$) when MEG3 was overexpressed, while overexpression of MEG3 had no effect on DNMT1 expression ($P > 0.05$).

Conclusions

Aberrant DNA methylation plays an important role in gene expression²¹. This study explored the regulatory role of MEG3/miR-494-3p/OTUD4 axis from the perspective of DNMT1 promoting MEG3 hypermethylation, so as to clarify the potential effect on the biological behaviors of breast cancer cells. Previous studies have demonstrated that DNMT1 (DNA methylase) can promote the methylation of lncRNA MEG3, and methylation of MEG3 promoter along with changes in gene region are the main reasons for abnormal expression of MEG3 in tumors²². Another study has shown that the treatment of glioma cells with the DNA methylation inhibitor (5'-Aza-2'-deoxycytidine) plays an important regulatory role in MEG3 expression²³. Aberrant methylation promoted by DNMT1 can increase the drug resistance of breast cancer cells to anticancer drugs. DNMT1 also promotes the development of breast cancer by reducing the expression of MEG3⁹. Therefore, this study verified the role of DNMT1 in regulating MEG3, and the results were consistent with previous reports. Further rescue experiments verified that knockdown of DNMT1 could demethylate MEG3 and promote its expression, thus inhibiting the proliferation, invasion and migration of breast cancer cells.

It is known that MEG3 can function as a ceRNA in tumors¹⁵. For example, MEG3 may regulate the progression of gastric cancer as a ceRNA binding to miR-181a²⁴, and regulate ischemic neuronal death by targeting miR-21/PDCD4 signaling pathway²⁵. MEG3 modulates EMT of cells by targeting miR-421 in breast cancer¹⁵. This study further explored the downstream targets of MEG3, and found that MEG3 could targeted bind to miR-494-3p. So, the RIP and dual-luciferase assays were used to verify their targeted binding relationship. The results implied that MEG3 could regulate the expression of miR-494-3p as a ceRNA. Zhou *et al.* have previously reported that miR-494-3p can promote cell proliferation and tumor growth in breast cancer through targeted inhibiting TRIM21 expression²⁶, and miR-494-3p has been found to inhibit self-renewal of breast cancer stem/progenitor cells²⁷, indicating the important regulatory role of miR-494-3p in breast cancer. In the study, we inhibited the cell activity, migration and invasion abilities of breast cancer cells by overexpression of MEG3. In the rescue experiments, overexpression of miR-494-3p reversed the inhibitory effect of MEG3 overexpression on the development of breast cancer cells. The results showed that overexpression of MEG3 could inhibit the proliferation, invasion and migration of breast cancer cells by targeted inhibiting miR-494-3p expression.

In order to further understand the regulatory mechanism, the target genes of miR-494-3p were predicted, and the downstream DE mRNAs in breast cancer were screened using GEO database. The results suggested that OTUD4 was poorly expressed in breast cancer tissue samples, and the 3'-UTR of OTUD4 could targeted bind to miR-494-3p. Then RIP and dual-luciferase assays were also used to verify their binding relationship, and the down-regulation of OTUD4 expression in miR-494-3p-overexpressing breast cancer cells was detected by western blot. This indicated that miR-494-3p targeted down-regulated the expression of OTUD4. OTUD4 has been found to be lowly expressed in non-small cell lung cancer and was able to inhibit the proliferation of cancer cells²⁸. In addition, alkylation damage which is critical for cancer chemotherapy can be regulated by OTUD4²⁹, but the mechanism of OTUD4 in breast cancer has not been reported. Rescue experiments were performed again to find that silencing OTUD4 reversed the inhibitory effects of miR-494-3p inhibitor on breast cancer cells. Moreover, the downstream regulatory effects of DNMT1 and MEG3 were further investigated to determine their impact on breast cancer progression.

In summary, we explored the role of DNMT1 in promoting MEG3 methylation, regulating the expression of genes in the MEG3/miR-494-3p/OTUD4 axis to influence the proliferation, migration and invasion of breast cancer cells. The study revealed the mutual interactions among MEG3, miR-494-3p and OTUD4, providing a new approach for targeted therapy of breast cancer.

Declarations

Ethics approval and consent to participate

Not applicable.

Consent for publication

Not applicable.

Availability of data and materials

The data and materials in the current study are available from the corresponding author on reasonable request.

Competing interests

The authors declare that they have no potential conflicts of interest.

Funding

Not applicable.

Authors' contributions

Xiaotao Zhu contributed to the study design. Fan Wang conducted the literature search and performed data analysis. Lin LV acquired the data and wrote the article. Mingzheng Wang and Chen Fan drafted. Xiaofeng Lu, Miaomiao Jin and Shuguang Li revised the article and gave the final approval of the version to be submitted. All authors read and approved the final manuscript.

Acknowledgements

Not applicable.

References

1. Sabatier R, Gonçalves A, Bertucci F. Personalized medicine: present and future of breast cancer management. *Crit Rev Oncol Hematol*. 2014;91:223–33. doi:10.1016/j.critrevonc.2014.03.002.
2. Chaffer CL, Weinberg RA. A perspective on cancer cell metastasis. *Science*. 2011;331:1559–64. doi:10.1126/science.1203543.
3. Jones PA. DNA methylation and cancer. *Oncogene*. 2002;21:5358–60. doi:10.1038/sj.onc.1205597.
4. Kastl L, Brown I, Schofield AC. Altered DNA methylation is associated with docetaxel resistance in human breast cancer cells. *Int J Oncol*. 2010;36:1235–41. doi:10.3892/ijo_00000607.
5. Rajabi H, et al. DNA methylation by DNMT1 and DNMT3b methyltransferases is driven by the MUC1-C oncoprotein in human carcinoma cells. *Oncogene*. 2016;35:6439–45. doi:10.1038/onc.2016.180.
6. Zhang W, et al. The correlation between DNMT1 and ER α expression and the methylation status of ER α , and its clinical significance in breast cancer. *Oncology letters*. 2016;11:1995–2000. doi:10.3892/ol.2016.4193.
7. Singh V, Sharma P, Capalash N. DNA methyltransferase-1 inhibitors as epigenetic therapy for cancer. *Curr Cancer Drug Targets*. 2013;13:379–99. doi:10.2174/15680096113139990077.
8. Li Z, et al. Long non-coding RNA H19 promotes the proliferation and invasion of breast cancer through upregulating DNMT1 expression by sponging miR-152. *J Biochem Mol Toxicol* 31, 10.1002/jbt.21933, doi:10.1002/jbt.21933 (2017).
9. Wang X-X, et al. miR-506 attenuates methylation of lncRNA MEG3 to inhibit migration and invasion of breast cancer cell lines via targeting SP1 and SP3. *Cancer cell international*. 2018;18:171–1. doi:10.1186/s12935-018-0642-8.
10. Zhou Y, Zhang X, Klibanski A. MEG3 noncoding RNA: a tumor suppressor. *J Mol Endocrinol*. 2012;48:R45–53. doi:10.1530/JME-12-0008.
11. Sun L, Li Y, Yang B. Downregulated long non-coding RNA MEG3 in breast cancer regulates proliferation, migration and invasion by depending on p53's transcriptional activity. *Biochem Biophys Res Commun*. 2016;478:323–9. doi:10.1016/j.bbrc.2016.05.031.
12. Zhang C-Y, et al. Overexpression of long non-coding RNA MEG3 suppresses breast cancer cell proliferation, invasion, and angiogenesis through AKT pathway. *Tumour biology: the journal of the*

- International Society for Oncodevelopmental Biology Medicine. 2017;39:1010428317701311–1. doi:10.1177/1010428317701311.
13. Liu X-H, et al. Lnc RNA HOTAIR functions as a competing endogenous RNA to regulate HER2 expression by sponging miR-331-3p in gastric cancer. *Mol Cancer*. 2014;13:92–2. doi:10.1186/1476-4598-13-92.
 14. Cesana M, et al. A long noncoding RNA controls muscle differentiation by functioning as a competing endogenous RNA. *Cell*. 2011;147:358–69. doi:10.1016/j.cell.2011.09.028.
 15. Zhang W, et al. LncRNA MEG3 inhibits cell epithelial-mesenchymal transition by sponging miR-421 targeting E-cadherin in breast cancer. *Biomedicine pharmacotherapy = Biomedecine pharmacotherapie*. 2017;91:312–9. doi:10.1016/j.biopha.2017.04.085.
 16. Wang H, et al. microRNA-21 promotes breast cancer proliferation and metastasis by targeting LZTFL1. *BMC Cancer*. 2019;19:738–8. doi:10.1186/s12885-019-5951-3.
 17. Li Z-Y, et al. The Long Noncoding RNA MEG3 and its Target miR-147 Regulate JAK/STAT Pathway in Advanced Chronic Myeloid Leukemia. *EBioMedicine*. 2018;34:61–75. doi:10.1016/j.ebiom.2018.07.013.
 18. Zhang X, Wu N, Wang J, Li Z. LncRNA MEG3 inhibits cell proliferation and induces apoptosis in laryngeal cancer via miR-23a/APAF-1 axis. *J Cell Mol Med*. 2019;23:6708–19. doi:10.1111/jcmm.14549.
 19. Wang M, et al. LncRNA MEG3-derived miR-361-5p regulate vascular smooth muscle cells proliferation and apoptosis by targeting ABCA1. *American journal of translational research*. 2019;11:3600–9.
 20. Roger M, et al. Treatment of precocious puberty with LH-RH agonists. Multicenter study using D-Trp-6-LH-RH in a programmed-release form. *Rev Fr Gynecol Obstet*. 1986;81:297–305.
 21. Si X, et al. ER α propelled aberrant global DNA hypermethylation by activating the DNMT1 gene to enhance anticancer drug resistance in human breast cancer cells. *Oncotarget*. 2016;7:20966–80. doi:10.18632/oncotarget.8038.
 22. Zhang X, et al. Maternally expressed gene 3 (MEG3) noncoding ribonucleic acid: isoform structure, expression, and functions. *Endocrinology*. 2010;151:939–47. doi:10.1210/en.2009-0657.
 23. Li J, et al. Epigenetic repression of long non-coding RNA MEG3 mediated by DNMT1 represses the p53 pathway in gliomas. *Int J Oncol*. 2016;48:723–33. doi:10.3892/ijo.2015.3285.
 24. Peng W, et al. Long non-coding RNA MEG3 functions as a competing endogenous RNA to regulate gastric cancer progression. *Journal of experimental clinical cancer research: CR*. 2015;34:79–9. doi:10.1186/s13046-015-0197-7.
 25. Yan H, et al. Long non-coding RNA MEG3 functions as a competing endogenous RNA to regulate ischemic neuronal death by targeting miR-21/PDCD4 signaling pathway. *Cell death disease*. 2017;8:3211–1. doi:10.1038/s41419-017-0047-y.
 26. Zhou W, et al. Decreased expression of TRIM21 indicates unfavorable outcome and promotes cell growth in breast cancer. *Cancer management research*. 2018;10:3687–96.

doi:10.2147/CMAR.S175470.

27. Chen S-M, et al. Hinokitiol up-regulates miR-494-3p to suppress BMI1 expression and inhibits self-renewal of breast cancer stem/progenitor cells. *Oncotarget*. 2017;8:76057–68. doi:10.18632/oncotarget.18648.
28. Wu Z, et al. OTU deubiquitinase 4 is silenced and radiosensitizes non-small cell lung cancer cells via inhibiting DNA repair. *Cancer cell international*. 2019;19:99–9. doi:10.1186/s12935-019-0816-z.
29. Zhao Y, et al. Noncanonical regulation of alkylation damage resistance by the OTUD4 deubiquitinase. *EMBO J*. 2015;34:1687–703. doi:10.15252/embj.201490497.

Tables

Table 1 Primer sequences

Genes	Primer sequences
miR-494-3p	F: 5'- GAAACATACACGGGAAAC C -3'
	R: 5'-GTGCAGGGTCCGAGG T-3'
U6	F:5'- CTCGCTTCG GCAGCACA-3'
	R:5'- AACGCTTCACGAATTTGC GT-3'
DNMT1	F: 5'- CGGCTTCAGCACCTCATTTG-3'
	R: 5'- AGGTCGAGTCGGAATTGCTC-3'
MEG3	F: 5'- ATCATCCGTCCACCTCCTTGTCTTC-3'
	R: 5'- GTATGAGCATAGCAAAGGTCAGGGC-3'
MSP-MEG3 (Methylation)	F: 5'- TATGAGTTGTAAGCGGTAGAGTTC-3'
	R: 5'- TACGAACTTAACGAAAAAAAAATCAT-3'
MSP-MEG3 (Non-methylation)	F: 5'- GAATATGAGTTGTAAGTGGTAGAGTTT-3'
	R: 5'- TACAACTTAACAAAAAAAAATCATACT-3'
OTUD4	F: 5'-TTCTGATGTGGATTACAGAGGGC-3'
	R: 5'- ACGCATGTTGTCTTACTCCTGA-3'
GAPDH	F: 5'-GAGTCAACGGATTTGGTCGT-3'
	R: 5'- TTGATTTTGGAGGGATCTCG-3'

Figures

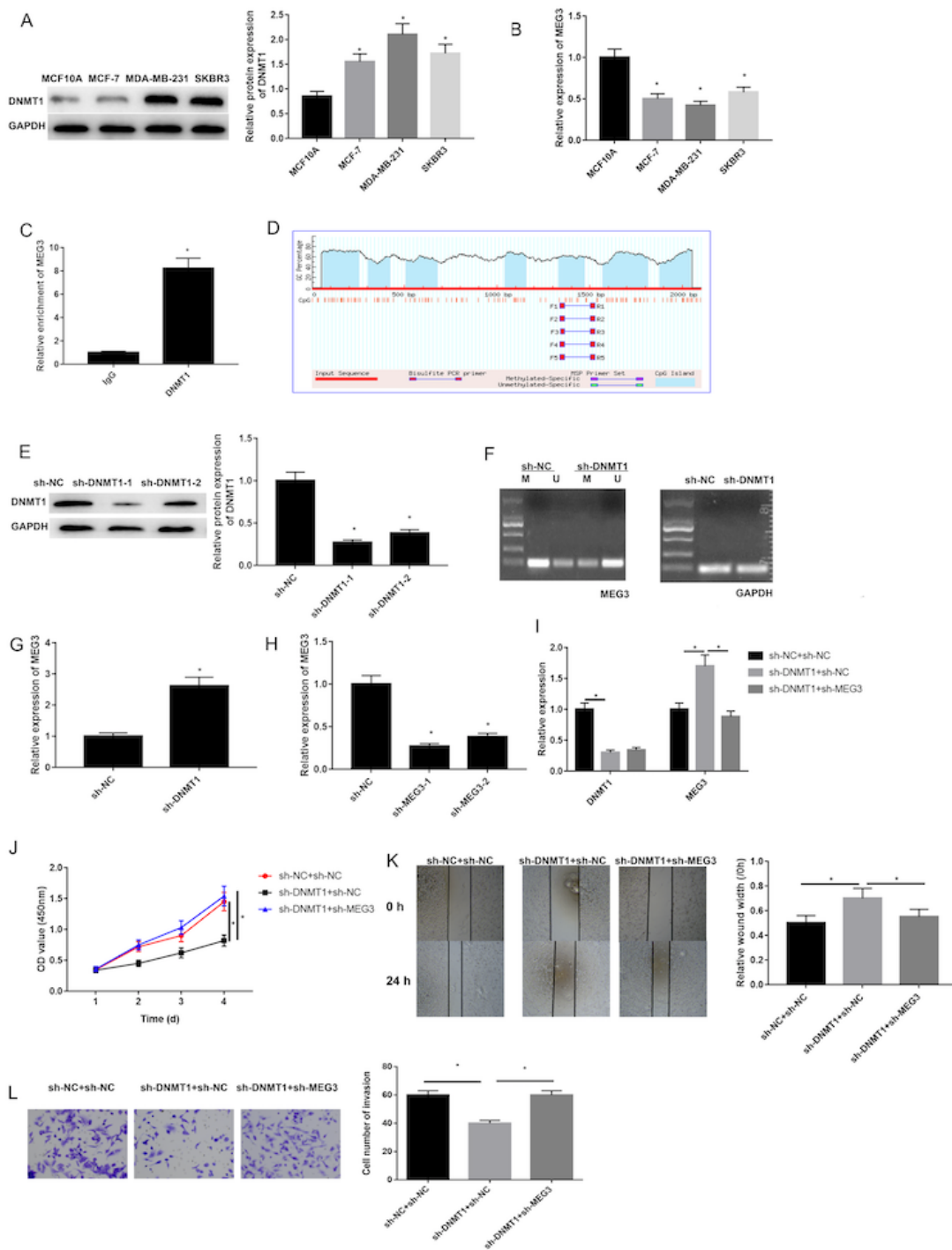


Figure 1

Silencing DNMT1 inhibits the proliferation, migration and invasion of breast cancer cells through promoting MEG3 expression. The expressions of (A) DNMT1 and (B) MEG3 in human breast cancer cell lines (MCF-7, MDA-MB-231, SKBR3) and human breast epithelial cell line MCF10A were detected by western blot and qRT-PCR, respectively; (C) ChIP assay was used to determine whether DNMT1 could bind to the promoter region of MEG3; (D) MEG3 methylation was determined by MethPrimer software and (F)

it methylation level was tested by MSP (U, unmethylated alleles; M, methylated alleles); (E) Western blot was used to detect the interference efficiency of DNMT1; (G) The expression of MEG3 was detected by qRT-PCR after DNMT1 was silenced; (H) Interference efficiency of MEG3 was detected by qRT-PCR; (I) The expressions of DNMT1 and MEG3 were detected by qRT-PCR in three groups (sh-NC+sh-NC, sh-DNMT1+sh-NC, sh-DNMT1+sh-MEG3); (J) Cell proliferation, (K) migration and (L) invasion abilities were tested by CCK-8, wound healing and Transwell assays, respectively. Each experiment was carried out in triplicate. (* P<0.05)

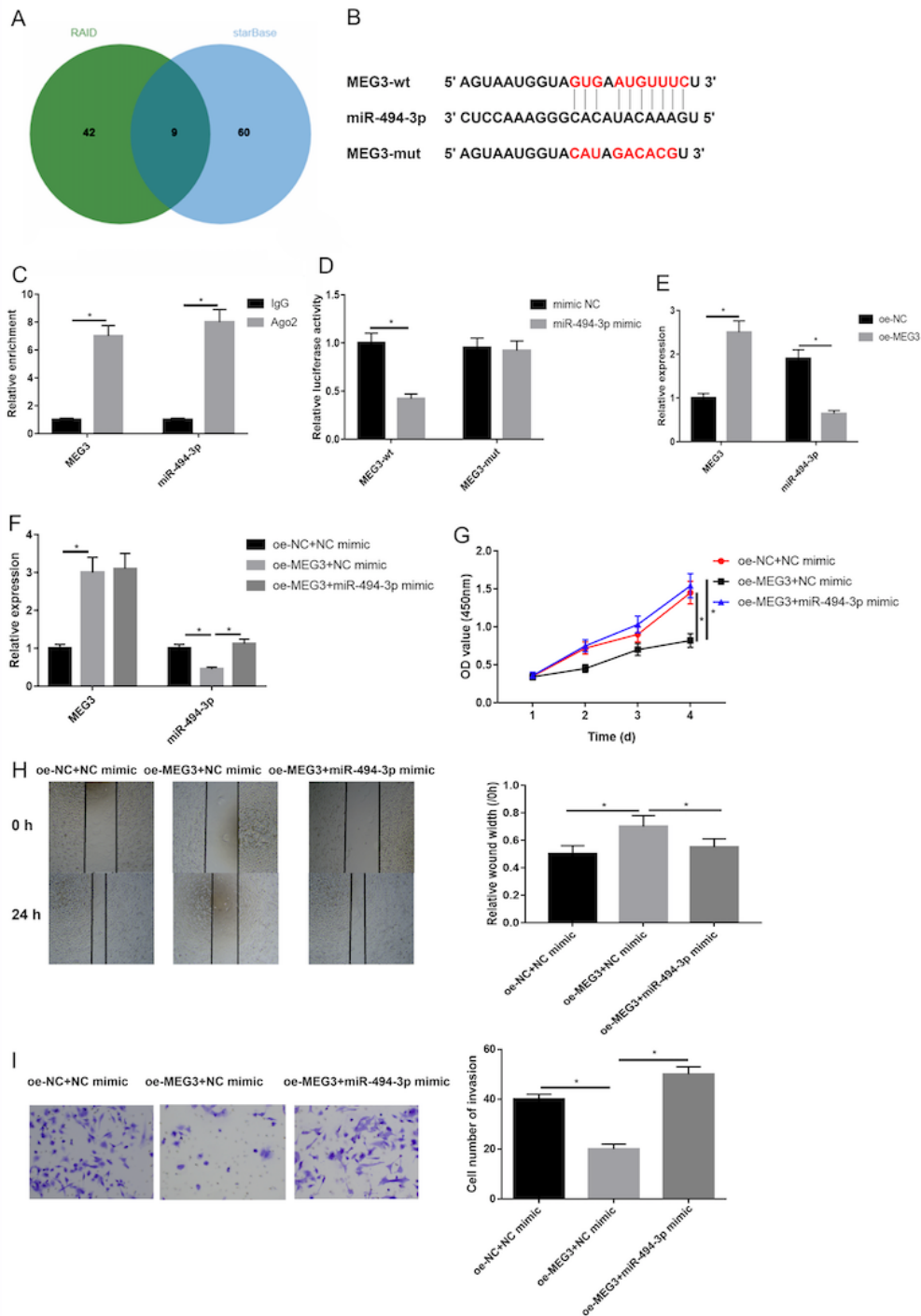


Figure 2

miR-494-3p is a target of MEG3 in breast cancer cells (A) The downstream miRNAs of MEG3 along with the (B) targeted binding sites of MEG3 and miR-494-3p were predicted by bioinformatics; (C) The binding relationship of MEG3 and miR-494-3p along with (D) binding sites were verified by RIP and dual-luciferase assays; (E) The expressions of MEG3 and miR-494-3p in sh-NC group and sh-MEG3 group were detected by qRT-PCR; (F) The expressions of MEG3 and miR-494-3p, (G) cell proliferation, (H) migration and (I) invasion abilities in oe-NC+NC mimic group, oe-MEG3+NC mimic group, and oe-MEG3+miR-494-3p mimic group were detected by qRT-PCR, CCK-8, wound healing and Transwell assays, respectively. Each experiment was carried out in triplicate. (* P<0.05)

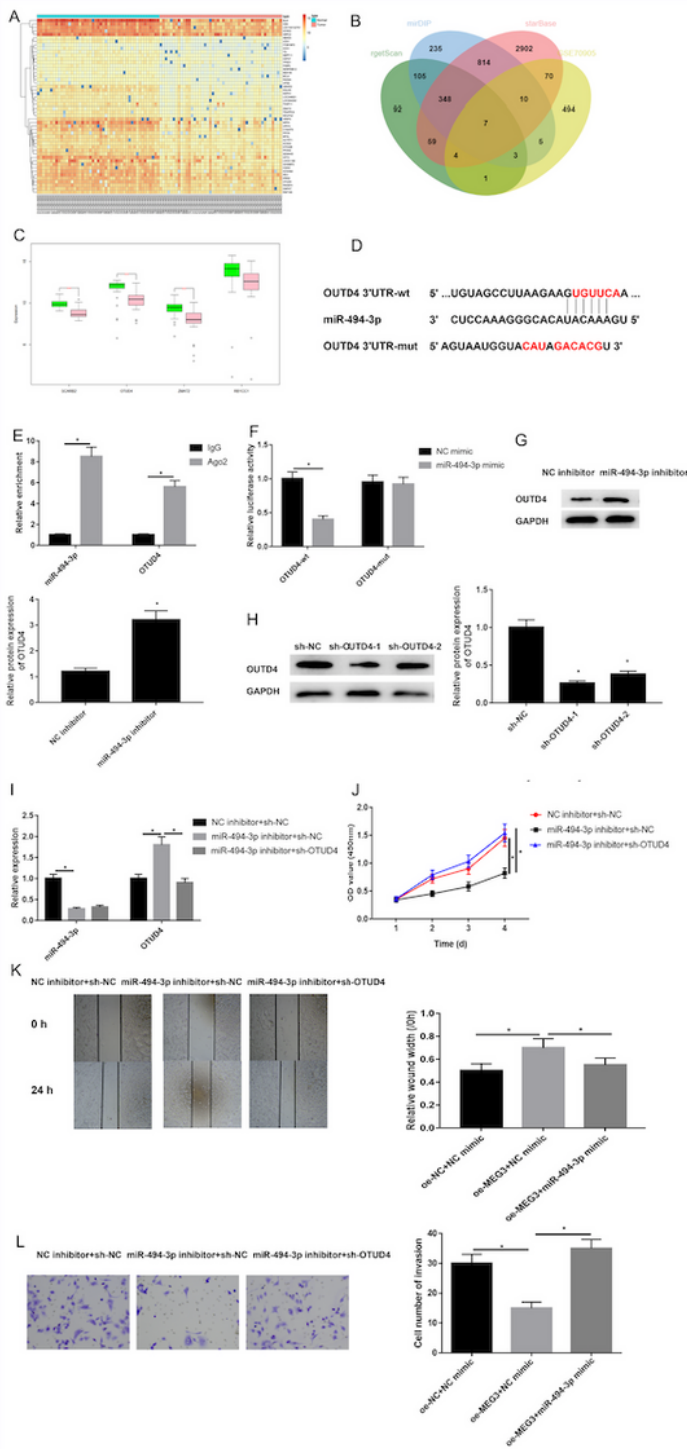


Figure 3

Silencing miR-494-3p can inhibit proliferation, migration and invasion of breast cancer cells by targeted promoting OTUD4 expression (A) DEGs in GS70905 dataset from GEO database were analyzed by bioinformatics; (B) Venn diagram of DEGs and predicted target genes of miR-494-3p; (C) Differential expression of candidate genes in GSE70905 dataset; (D) The targeted binding sites of MEG3 and miR-494-3p were predicted by starBase database; (E) RIP and (F) dual luciferase assays were performed to

verify the targeted binding relationship between miR-494-3p and OTUD4; (G) The expression of OTUD4 in NC inhibitor and miR-494-3p inhibitor group was detected by western blot; (H) OTUD4 interference efficiency was tested by western blot; (I) The expressions of miR-494-3p and OTUD4, (J) cell proliferation, (K) migration and (L) invasion abilities in NC inhibitor+sh-NC, miR-494-3p inhibitor+sh-NC, and miR-494-3p inhibitor+sh-OTUD4 groups were measured by qRT-PCR, CCK-8, wound healing and Transwell assays, respectively. Each experiment was carried out in triplicate. (* $P < 0.05$)

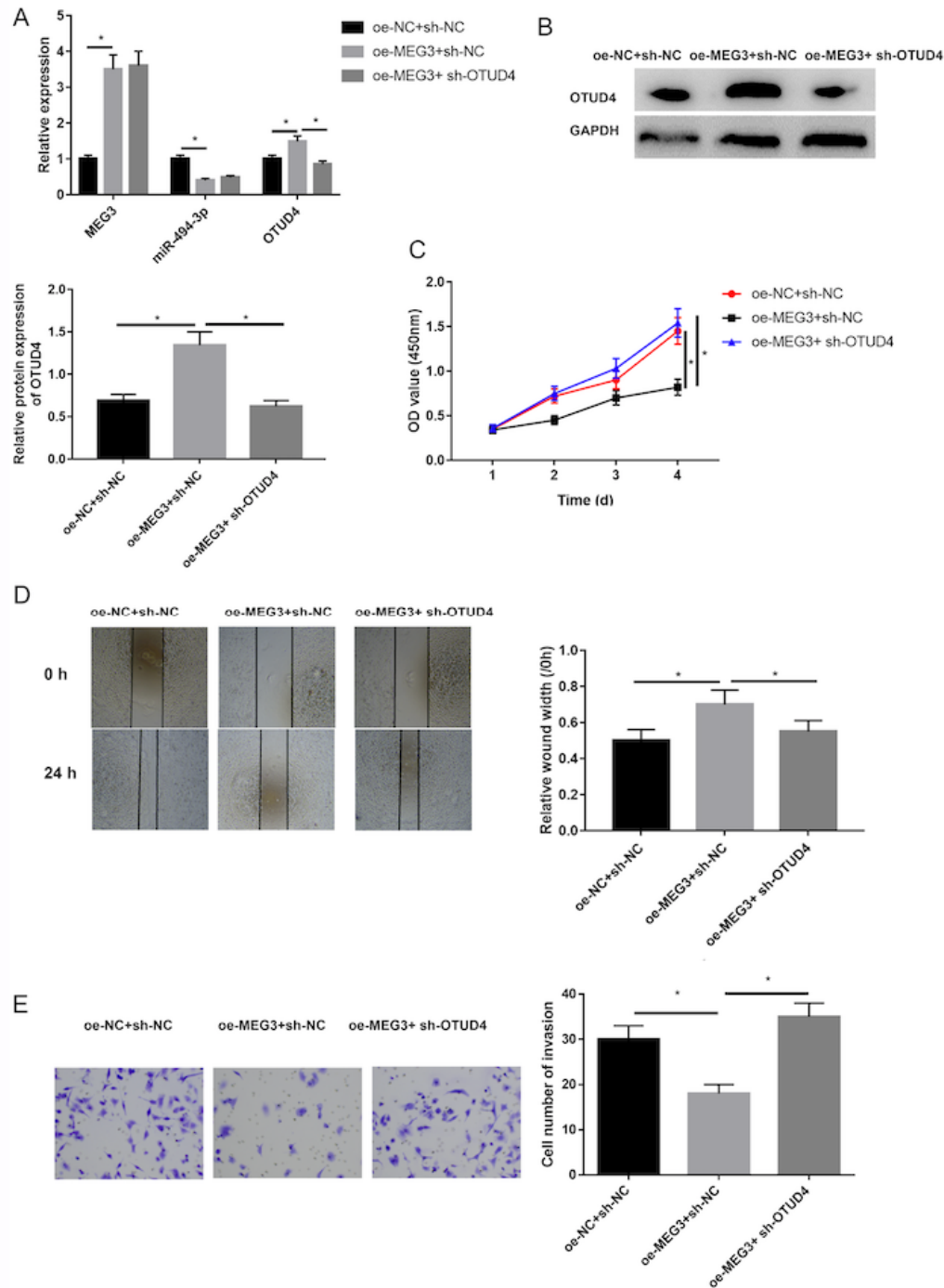


Figure 4

MEG3 negatively regulates miR-494-3p to promote OTUD4 expression and inhibit the proliferation, migration and invasion of breast cancer cells (A) The expressions of MEG3, miR-494-3p and OTUD4 in oe-NC+sh-NC, oe-MEG3+sh-NC and oe-MEG3+sh-OTUD4 groups were detected by qRT-PCR and (B) the protein expression of OTUD4 was tested by western blot; (C) Cell proliferation, (D) migration and (E) invasion abilities were measured by CCK-8, wound healing and Transwell assays, respectively. Each experiment was carried out in triplicate.. (* P<0.05)

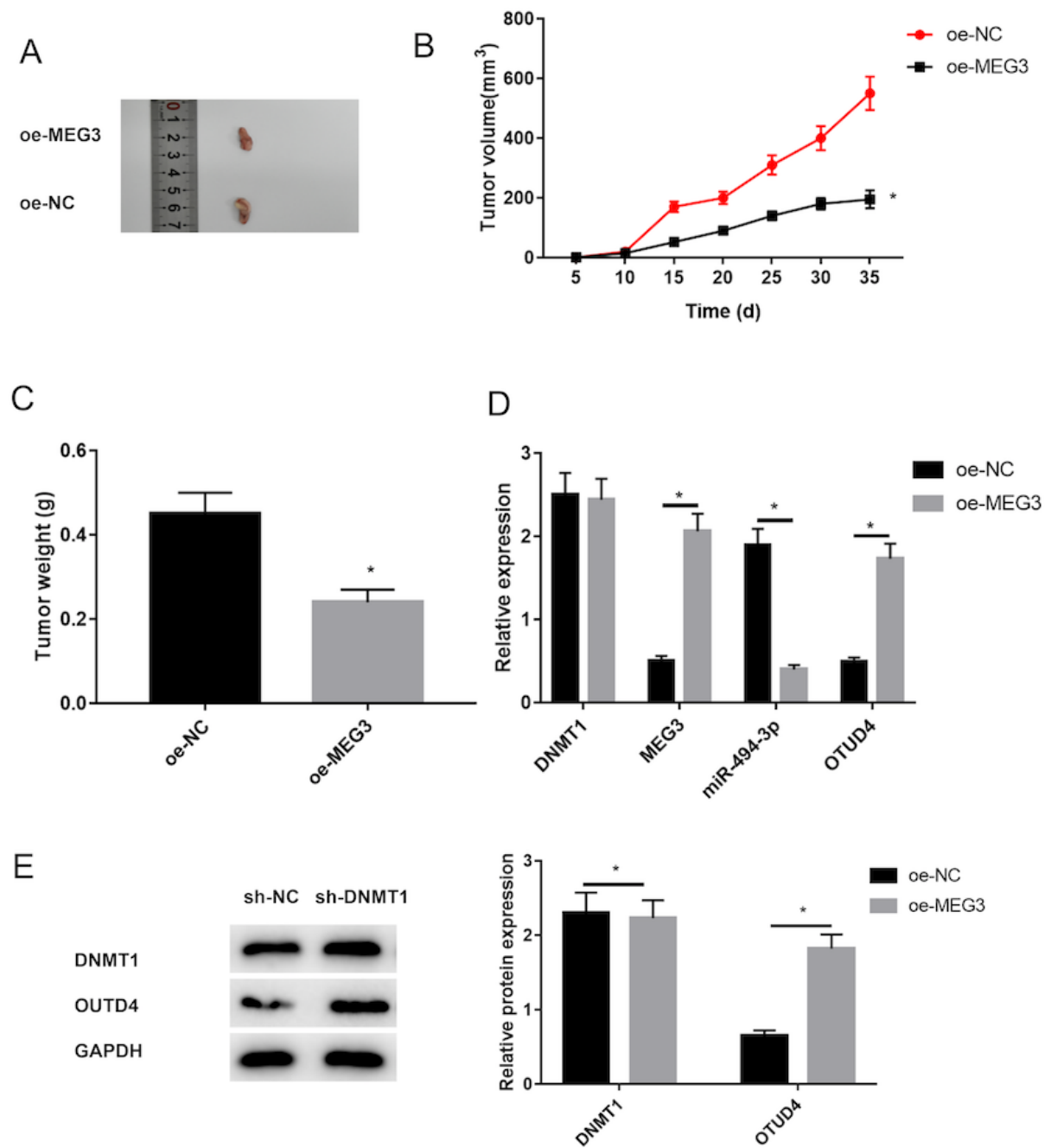


Figure 5

Silencing DNMT1 inhibits breast cancer cell tumorigenesis in vivo (A) Tumor stereogram, (B) volume and (C) weight of nude mice in each group were measured; (D) The expressions of DNMT1, MEG3, miR-494-3p and OTUD4 were detected by qRT-PCR and (E) the protein expression of DNMT1 and OTUD4 was test by western blot. Each experiment was carried out in triplicate. . (* P<0.05)